Size dependence of strain relaxation and lateral quantization in deep etched $Cd_xZn_{1-x}Se/ZnSe$ quantum wires

T. Kümmell,* G. Bacher, and A. Forchel
Technische Physik, Universität Würzburg, Am Hubland, D-97074 Würzburg, Germany

G. Lermann and W. Kiefer
Institut für Physikalische Chemie, Universität Würzburg, Am Hubland, D-97074 Würzburg, Germany

B. Jobst,† D. Hommel,† and G. Landwehr
Experimentelle Physik III, Universität Würzburg, D-97074 Würzburg, Germany

(Received 23 October 1997)

A systematic experimental and theoretical analysis of the lateral size and composition dependence of strain release and lateral quantization in etched $Cd_xZn_{1-x}Se/ZnSe$ quantum wires is presented. Wires with lateral structure sizes down to 14 nm were realized by electron beam lithography and wet chemical etching and characterized by photoluminescence (PL) and Raman spectroscopy. For wide wires ($L_x>40$ nm), the strain relaxation results in a redshift of both the energy of the PL signal and the $Cd_xZn_{1-x}Se$ LO phonon frequency in the wire region. To model the strain release, theoretical calculations have been performed, minimizing the elasticity energy in the wire cross section. A size-dependent strain release, strongly inhomogeneous across the wire cross section, is obtained. This results in a size- and composition-dependent band-gap shift, which is found to be in good agreement with the experimental data. In narrow wires ($L_x<30$ nm), the Raman data indicate a saturation of the strain release. As a consequence, clear lateral quantization effects due to the quasi-one-dimensional carrier confinement are observed in the PL spectrum, resulting in a blueshift of the PL signal with decreasing wire width. [S0163-1829(98)04424-5]

I. INTRODUCTION

Strain in epitaxially grown semiconductor heterostructures is a consequence of the combination of compounds with different lattice constants. Modern growth techniques such as, e.g., molecular beam epitaxy (MBE) or metal-organic vapor phase epitaxy (MOVPE) allow the realization of high quality elastically strained heterostructures, if the thickness of the strained layers is kept below a certain critical thickness.[1] On the one hand, this allows the design of a wide variety of semiconductor heterostructures. On the other hand, the strain can be used intentionally to modify fundamental electronic and optical properties like the band gap, the splitting between heavy and light holes, the hole masses, and the density of states, and therefore, e.g., to improve the performance of laser diodes.[2–5] Thus strain effects in quasi-two-dimensional epilayers have been investigated widely both by experiment and theoretically.[6–10]

The growing attention to the properties of quantum wires and quantum dots in recent years has resulted in new questions concerning the lattice strain in low-dimensional structures. In quasi-one-dimensional (quasi-1D) or quasi-zero-dimensional structures the strain is expected to change with respect to 2D layers, because the sidewalls can relax partially in deep etched patterns[11–13] or are affected by an additional lateral change of the lattice constant in buried nanostructures.[14,15] De Caro and Tapfer have published a theoretical investigation assuming homogeneous strain in wires and solving the problem analytically for different substrate and wire orientations.[16] On the other hand, it has been observed that strain release in wires shows a high nonuniformity in both overgrown[17] and deeply etched structures.[12] Model calculations and Raman experiments at freestanding stripe films confirm these results.[18,19] In their comprehensive work on overgrown quantum wires, Notomi *et al.* extrapolated calculated strain fields to obtain band-gap changes in the $In_xAs_{1-x}P/InAs$ system, explaining the experimentally observed blueshift of the photoluminescence (PL) signal with decreasing wire width.[14] Similar effects have been investigated experimentally and theoretically for buried dots and wires based on InAs/GaAs, InP/GaAs, or InP/InGaP.[15,20] Because in these overgrown structures both strain and lateral carrier confinement are responsible for a blueshift of the bandgap with decreasing wire width, it is difficult to distinguish experimentally between quantization and strain effects. In contrast, in deeply etched $Cd_xZn_{1-x}Se/ZnSe$ wires the strain release causes a redshift of the signal with decreasing wire width[11,13] and can be clearly separated from confinement effects, which are observed only in narrow quantum wires due to the high carrier masses.[21] The lattice mismatch between CdSe and ZnSe is quite substantial (about 6.7%) and very high quality heterostructures are available because of the application potential of this system for blue-green emitting laser diodes.[22,23] Hence, deep etched $Cd_xZn_{1-x}Se/ZnSe$ quantum wires represent an ideal model system to study the influence of strain release as well as lateral carrier confinement on the optical properties of strained nanostructures.

In this work a systematic experimental and theoretical investigation of strain release in deeply etched $Cd_xZn_{1-x}Se/ZnSe$ wire structures is presented. The technology of electron beam lithography and wet chemical etching

 © 1998 The American Physical Society

for the wire fabrication allows a well defined variation of the lateral wire size. Photoluminescence and Raman spectroscopy were performed in order to get experimental access to both the change of the band gap and the LO phonon frequency as a consequence of the size-dependent lattice distortion. The strain fields are modeled theoretically by minimizing the lattice strain energy in deep etched wire structures. We discuss the calculated strain distribution and the resulting variation of the band gap across the wire cross section and the consequences to the optical properties of the wire structures and compare the predicted effects with experimental data.

II. SAMPLE PREPARATION AND EXPERIMENT

Single quantum well (SQW) heterostructures have been grown by molecular beam epitaxy in a two chamber Riber 2300 system on a (001)-oriented GaAs substrate using a 200 nm GaAs buffer layer to guarantee high sample quality. Sample A was grown with a 620 nm $ZnS_{0.06}Se_{0.94}$ buffer, latticed matched to the GaAs substrate, a 50 nm ZnSe layer, a 5.5 nm $Cd_{0.35}Zn_{0.65}Se$ well, and covered by a 13 nm ZnSe cap layer. Sample B consists of a 70 nm ZnSe barrier, a 5.5 nm $Cd_{0.12}Zn_{0.88}Se$ well, and a 15 nm ZnSe cap layer. As the lattice constants of CdSe, ZnSe, and GaAs are 6.052 Å, 5.668 Å, and 5.653 Å, respectively,[24] it is important to keep the total layer thickness of the $Cd_xZn_{1-x}Se$/ZnSe structure below the critical layer thickness.[25] The pseudomorphic growth was confirmed by high resolution x-ray diffraction.[26] Both the ZnSe barrier and the $Cd_xZn_{1-x}Se$ well are compressively strained in the ⟨100⟩ and the ⟨010⟩ direction.

The samples were coated with polymethylmethacrylate (PMMA) resist, and wire patterns were defined by electron beam lithography. The resist was developed and a 15 nm thick Ti layer was evaporated. After resist lift-off, the Ti patterns serve as etch masks. In order to obtain high quantum efficiencies down to the narrowest wires, the pattern transfer was performed by wet chemical etching using a $K_2Cr_2O_7/HBr/H_2O$ solution.[21] The etch depth was about 70 nm. A characteristic feature of this wet etch process is a strong dependence of the etch profile on the wire orientation with respect to the substrate. In order to obtain vertical sidewalls in the vicinity of the $Cd_xZn_{1-x}Se$ well the wires are oriented parallel to the ⟨110⟩ direction.[27] 70×70 μm^2 arrays with lateral wire sizes between 14 nm and 500 nm were realized on each sample as well as some 2D reference (mesa) fields. This enables us to obtain PL and Raman data as a function of the wire width in direct comparison with a two-dimensional reference from each sample.

The structures were characterized by low temperature photoluminescence and Raman spectroscopy. For the PL measurements at 2 K, the samples were placed into a liquid helium cryostat. The 363.8 nm line of an Ar^+ laser was used for excitation. The excitation density was varied between 2 mW/cm^2 and 100 W/cm^2. The PL signal was dispersed by a monochromator with a focus length of 0.32 m and detected with a charge coupled device (CCD) camera. The Raman measurements were performed using a micro Raman setup with a microscope objective at a working distance of 4.2 mm that enabled us to focus the laser to an area of about 0.8 μm^2. The sample was placed in a closed cycle cryostat at a temperature of 9 K. For these experiments the excitation wavelength of the Ar^+ laser was 472.7 nm and the excitation power was about 5 mW. The scattered Raman signal was detected by a double monochromator equipped with a CCD camera.

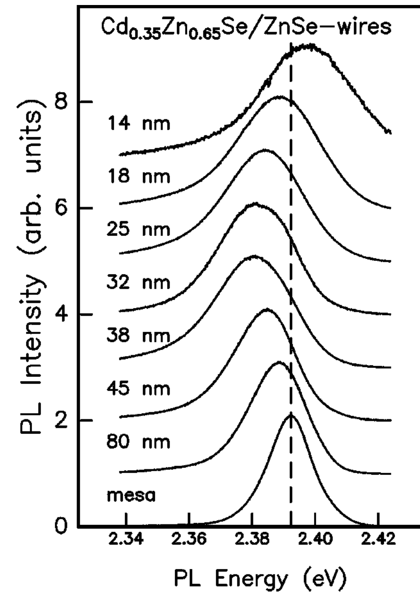

FIG. 1. PL spectra of deeply etched $Cd_{0.35}Zn_{0.65}Se$/ZnSe wire arrays with lateral width $L_x>32$ nm (left side) and $L_x\leqslant32$ nm (right side).

III. OPTICAL CHARACTERIZATION OF THE WIRES

In order to investigate the shift of the band gap with decreasing wire width, we performed PL measurements. In Fig. 1, low temperature ($T=2$ K) PL spectra of sample A ($Cd_{0.35}Zn_{0.65}Se$/ZnSe SQW) for a quasi-two-dimensional reference (mesa) and quantum wires with different widths are plotted. The intensity is normalized to the 2D reference and the spectra are shifted vertically for clarity. As a striking result, we see two regimes with opposite behavior. Starting with the 2D reference and reducing the wire size, a continuous shift of the PL maximum to lower energies is observed. For a wire width of about 32 nm, this shift has reached its maximum with a peak energy of the PL signal, which is redshifted by about 11 meV compared to the 2D reference. Decreasing the wire size further, a strong increase of the PL energy is observed, which amounts to 17 meV between a 32 nm and a 14 nm wide wire. The complicated size dependence of the PL energy indicates that at least two different effects have to be taken into account in order to explain the experimental data quantitatively. On the one hand, the biaxial strain in the epitaxial $Cd_xZn_{1-x}Se$ layer increases the band gap compared to bulk $Cd_xZn_{1-x}Se$.[8] Therefore in the etched structures strain relaxation results in a systematic shift of the wire luminescence to lower energies with decreasing wire width.[11,13] On the other hand, the blueshift of the PL signal observed for the narrowest wires is attributed to lateral carrier confinement.[21,27] Both effects will be discussed later in more detail.

A more direct experimental access to the lattice distortion by strain release is given by Raman spectroscopy. As the LO

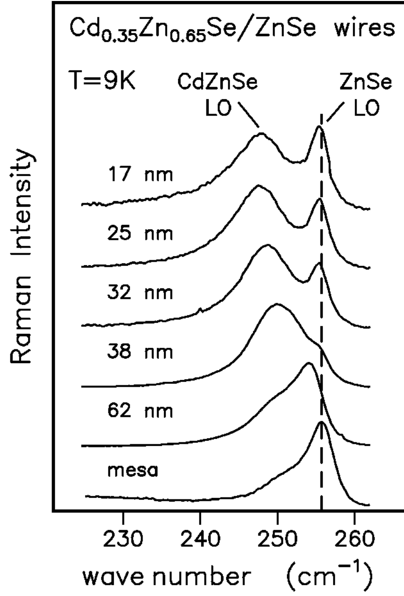

FIG. 2. Raman spectra of deeply etched $Cd_{0.35}Zn_{0.65}Se/ZnSe$ wire arrays.

phonon frequency strongly depends on the lattice constant, a change of the lattice constant due to strain release should result in a shift of the LO phonon frequency.[28] We have analyzed the same sample as discussed above by micro Raman measurements, probing the wire width dependence of the LO phonon energy. Figure 2 shows Raman spectra for different wire widths at $T=9$ K compared to the 2D reference. For both mesa and wires two characteristic Raman signals are observed. The peak at about 256 cm^{-1} is detected on the wire arrays as well as between the patterned fields and corresponds to the LO phonon of the ZnSe barrier material, with an energy nearly independent of the wire width. The second signal is only obtained by focusing the laser beam onto the wire arrays and thus is attributed to the LO phonon of the $Cd_xZn_{1-x}Se$ wire. In accordance with former measurements,[29] no separate CdSe LO phonon mode is found. In the case of the 2D reference the $Cd_xZn_{1-x}Se$ related Raman peak is only detected as a shoulder at the low energy side of the ZnSe signal. With decreasing lateral wire size the $Cd_xZn_{1-x}Se$ phonon shifts further towards lower energies and becomes clearly separable from the ZnSe LO peak. As a shift of the Raman signal of the $Cd_xZn_{1-x}Se$ wires directly reflects the influence of the lattice deformation due to a variation of the strain,[19,28] these results are attributed to a release of the compressive strain in the wires for decreasing lateral size. For wires below 30 nm, however, no further shift of the LO peak is obtained, indicating a saturation of the strain release in narrow wires.

IV. THEORETICAL MODELING OF THE STRAIN RELAXATION

In order to describe the strain relaxation process in the wires quantitatively we have used elasticity theory. As mentioned before, heteroepitaxial structures are strained in the case of a lattice mismatch between the different layers and a pseudomorphic growth. The latter point is of particular importance, as a model applying elasticity theory can only be valid for a layer structure free from dislocations and with clearly defined lattice constants. The samples investigated in this work consist of ZnSe and $Cd_xZn_{1-x}Se$ layers, grown lattice matched to GaAs on a GaAs substrate with a GaAs buffer (sample B) and a GaAs/$Zn_xS_{1-x}Se$ buffer (sample A). The lattice mismatches with respect to the GaAs substrate, defined as $(a_{\mathrm{substrate}}-a_{\mathrm{layer}})/a_{\mathrm{layer}}$ (unstrained lattice constants) are -0.26%, -2.57%, and -1.07% for the ZnSe barrier, the quantum well in sample A, and the quantum well in sample B, respectively. The negative signs indicate compressive strain for both the $Cd_xZn_{1-x}Se$ quantum well and the ZnSe barrier.

With z parallel to the growth direction and the quantum well in the x-y plane, the in-plane strain for the ZnSe barrier and the $Cd_xZn_{1-x}Se$ well is

$$\epsilon_{xx}^{\mathrm{ZnSe}}=\epsilon_{yy}^{\mathrm{ZnSe}}=(a_{\mathrm{GaAs}}-a_{\mathrm{ZnSe}})/a_{\mathrm{ZnSe}}$$

and

$$\epsilon_{xx}^{\mathrm{Cd}_x\mathrm{Zn}_{1-x}\mathrm{Se}}=\epsilon_{yy}^{\mathrm{Cd}_x\mathrm{Zn}_{1-x}\mathrm{Se}}=(a_{\mathrm{GaAs}}-a_{\mathrm{Cd}_x\mathrm{Zn}_{1-x}\mathrm{Se}})/a_{\mathrm{Cd}_x\mathrm{Zn}_{1-x}\mathrm{Se}},$$

respectively. Because no restriction is applied to the growth (z) direction, the strain in this direction is determined by the Poisson ratio σ: $\epsilon_{zz}^{\mathrm{ZnSe}}=-\epsilon_{xx}^{\mathrm{ZnSe}}/\sigma_{\mathrm{ZnSe}}$ in the barrier and $\epsilon_{zz}^{\mathrm{Cd}_x\mathrm{Zn}_{1-x}\mathrm{Se}}=-\epsilon_{xx}^{\mathrm{Cd}_x\mathrm{Zn}_{1-x}\mathrm{Se}}/\sigma_{\mathrm{Cd}_x\mathrm{Zn}_{1-x}\mathrm{Se}}$ in the quantum well.[14] As $\sigma>0$, the compressive in-plane strain is counterbalanced by a tensile strain perpendicular to the plane. All shear strain components ϵ_{xy}, ϵ_{yz}, ϵ_{zx} are equal to zero in the 2D material.

In a quasi-one-dimensional, deep etched wire structure the situation changes fundamentally. The wire sidewalls represent additional free surfaces where the structure is free from the constraints given in the 2D structure. As a consequence, the structure undergoes a partial strain relaxation at least in the vicinity of the sidewalls, reducing the strain energy. In order to get quantitative information on the strain relaxation, we have to minimize numerically the strain energy in the wire. The following coordinates are used: z indicates the growth direction $\langle 001\rangle$, y is parallel to the wire direction $\langle 110\rangle$, and x describes the direction perpendicular to the wires $\langle 1\bar{1}0\rangle$.

In a solid, the strain energy of a deformed volume element is given by

$$W=\frac{1}{2}\sum_{i,j=1}^{6} c_{ij}\epsilon_i\epsilon_j, \tag{1}$$

where

$$\epsilon_1=\epsilon_{xx},\quad \epsilon_2=\epsilon_{yy},\quad \epsilon_3=\epsilon_{zz},$$
$$\epsilon_4=\epsilon_{yz},\quad \epsilon_5=\epsilon_{zx},\quad \epsilon_6=\epsilon_{xy},$$

and the c_{ij} are the elastic constants in the (x,y,z) coordinate system, i.e., the C_{ij} for ZnSe (Ref. 24) have to be transferred from the crystal lattice axes to our coordinate system.[19] To calculate the strain in a wire, we assume a rectangular wire profile, i.e. vertical sidewalls in the vicinity of the $Cd_xZn_{1-x}Se$ layer. As the strain in the wire direction ϵ_{yy} does not change and ϵ_{xy} and ϵ_{yz} are zero, the problem can be reduced to two dimensions. We are subdividing the wire cross section (x-z plane) into a two-dimensional grid. The evaluation of ϵ_{xx}, ϵ_{zz}, and ϵ_{zx} as functions of (x,z) completely characterizes the strain field in the wire. The strain energy of each grid point with respect to its neighbors was minimized according to Eq. (1). This procedure was repeated

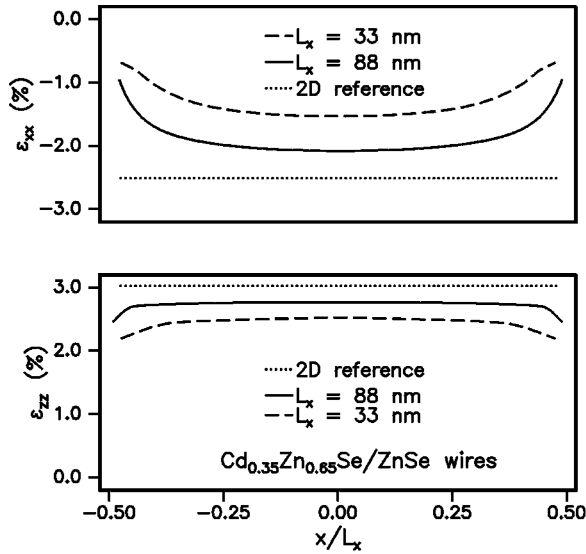

FIG. 3. Strain in the center of a $Cd_{0.35}Zn_{0.65}Se/ZnSe$ layer for 2D layer (dotted line), an 88 nm wide wire (solid line), and a 33 nm wide wire (dashed line) as a function of the lateral position x in the wire: [(a), top] Strain perpendicular to growth direction and wire orientation, ϵ_{xx}. [(b), bottom] Strain in growth direction, ϵ_{zz}.

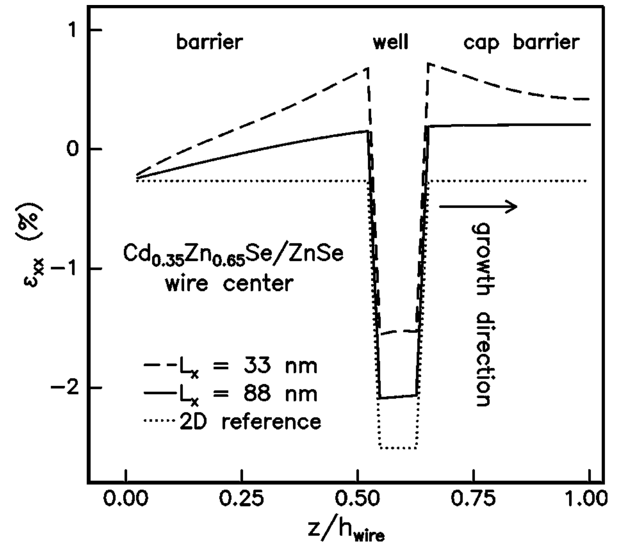

FIG. 4. Strain in the center of the wire for a 2D reference (dotted line), an 88 nm wide wire (solid line), and a 33 nm wide wire (dashed line) as a function of the position along the growth direction z. The curves refer to the $Cd_{0.35}Zn_{0.65}Se/ZnSe$ system.

until the minimum of the total strain energy in the wire was obtained, resulting in ϵ_{xx}, ϵ_{zz}, and ϵ_{zx} as functions of (x,z).

To discuss the results of our model calculations, we will first concentrate on sample A. The exact sample design, i.e., the well and the barrier thickness as well as the Cd content of the well, has been determined by x-ray diffraction measurements.[26] We evaluated the strain fields $\epsilon_{ij}(x,z)$ for different wire widths and compared it to the quasi-two-dimensional reference. As the strain field is only determined by the ratio between the well thickness and the wire width, the results can be easily transferred to other quantum well thicknesses.

To give an impression of how the strain field changes with decreasing wire size, ϵ_{xx} in the center of the quantum well (i.e., z=const) is depicted in Fig. 3(a) for different wire widths as a function of x. The dotted line describes the situation in the 2D reference, where ϵ_{xx} amounts to -2.51% due to the uniform compressive strain. In the 88 nm wide wire (solid line), the absolute value of ϵ_{xx} is reduced, caused by a release of the compressive in-plane strain. The figure shows that the increase of the in-plane lattice constant of the $Cd_xZn_{1-x}Se$ wire is most important at the sidewalls. This is easy to understand, because in the vicinity of the open sidewalls the relaxation process is expected to be most efficient. Reducing the wire width to 33 nm (dashed line), the relaxation process has proceeded further, resulting in a residual strain ϵ_{xx} in x direction of -1.6% in the center of the wire. However, the strain field at the sidewall is quite independent of the wire width. Hence, the difference between the strain at the sidewalls and in the center of the wire is more pronounced in wide wires. There are typically 5–10 nm wide regions at the sidewalls, where a strongly inhomogeneous strain field is obtained.

For comparison, Fig. 3(b) shows ϵ_{zz} in the center of the quantum well as a function of x. In the 2D case (dotted line), there is a uniform tensile strain of ϵ_{zz}, which is about 3.02%. The strain relaxation occurring in the wires results in a reduction of the tensile strain of the $Cd_xZn_{1-x}Se$ layer, which is not surprising, because the tensile strain in the growth direction was caused by the compressive in-plane strain, as mentioned above. Therefore, as in Fig. 3(a), the relaxation process is most pronounced at the sidewalls. However, the strain relaxation in z direction is less distinct than the change of ϵ_{xx}. For instance, in wires of L_x=88 nm (solid line) and L_x=33 nm (dashed line), ϵ_{zz} in the center of the wire is only reduced to about 2.8% and 2.4%, respectively.

Because no dislocations are induced at the barrier-well interface, the strain release in the wires results in a modification of the strain field in the barriers. This is illustrated in Fig. 4, where ϵ_{xx} is plotted as a function of z, while x is kept constant in the center of the well. The etch depth, i.e., the height of the wire, is $h_{\rm wire}$. The dotted line describes the 2D reference, where the barrier has a compressive strain of -0.26% and the quantum well a compressive strain of -2.51%, as mentioned above. In the case of a narrow (L_x =33 nm) wire (dashed line), the strain release results in a reduction of the compressive strain in the $Cd_xZn_{1-x}Se$ layer from -2.51% to about -1.6%. In addition, the barrier undergoes a tensile deformation, which is particularly strong in the vicinity of the barrier-well interface. From an energetic point of view, a fraction of the strain energy in the quantum well region is transmitted to the barrier regions, and eventually a balance of deformation between barrier and well with a minimal total energy is achieved. It has to be noted that because of the small cap layer thickness, even the top of the wire is influenced by the strain release, resulting in a tensile strain of the ZnSe cap layer. As expected, in the center of an 88 nm wide wire (solid line), both strain release in the quantum well and the tensile strain in the barrier reveal an intermediate state between the mesa reference and the narrow wire. In addition to the size-dependent strain ϵ_{xx} and ϵ_{zz}, the distortion causes a shear strain component ϵ_{zx} especially pronounced at the wire sidewalls and at the quantum-well–barrier interface.

In order to compare the PL data with our theory, the cal-

TABLE I. Deformation potentials a_c, a_v, a, b, and d, Luttinger parameters γ_1 and γ_2, electron mass m_e, and in-plane heavy hole mass $m_{\mathrm{hh},\parallel}$ for ZnSe and CdSe in zinc-blende formation. The values for the ternary compounds are obtained by a linear interpolation.

	CdSe	ZnSe	$Cd_{0.35}Zn_{0.65}Se$	$Cd_{0.12}Zn_{0.88}Se$
a_c (eV)	−3.13[a]	−5.9[b]	−4.9	−5.57
a_v (eV)	−0.53[a]	−1.0[b]	−0.84	−0.94
$(a=a_c-a_v)$ (eV)	−2.6	−4.9	−4.06	−4.63
b (eV)	−0.7[c]	−1.14[d]	−0.99	−1.09
d (eV)		−3.8[c]		
γ_1	1.9[a]	2.45[e]		
γ_2	0.75[a]	0.61[e]		
m_e/m_0	0.11[f]	0.145[a]	0.133	0.141
$m_{hh,\parallel}/m_0$	0.38	0.33	0.345	0.334

[a]Reference 32.
[b]Reference 35.
[c]Reference 31.
[d]Reference 36.
[e]Reference 37.
[f]Reference 24.

culated strain fields in the partially relaxed wires have to be transferred to a variation of the band gap. We define primed coordinates (x',y',z'), that follow the $\langle 100\rangle$, $\langle 010\rangle$, and $\langle 001\rangle$ directions of the crystal, respectively, and solve the strain Hamiltonian at $k=0$. Primed ϵ'_{ij} are introduced as abbreviations for $\epsilon_{i'j'}$ referring to the (x',y',z') coordinate system. As the wires are orientated in $\langle 110\rangle$ direction, and $\epsilon_{xy}=\epsilon_{yz}=0$, the transformation from the wire coordinate system (x,y,z) to the crystal coordinate system (x',y',z') is performed by

$$\epsilon'_{yz}=\epsilon'_{zx}=\epsilon_{zx}/\sqrt{2}, \quad \epsilon'_{xy}=(\epsilon_{xx}-\epsilon_{yy})/2, \qquad \epsilon'_{xx}=\epsilon'_{yy}=(\epsilon_{xx}+\epsilon_{yy})/2. \tag{2}$$

According to Pikus and Bir[30] the change of the energy of the conduction and the valence band, respectively, due to strain is

$$\Delta E_c=a_c(\epsilon'_{xx}+\epsilon'_{yy}+\epsilon'_{zz}), \qquad \Delta E_v^{\mp}=a_v(\epsilon'_{xx}+\epsilon'_{yy}+\epsilon'_{zz})\pm\sqrt{\frac{b^2}{2}S+d^2T}, \tag{3}$$

where

$$S=(\epsilon'_{xx}-\epsilon'_{yy})^2+(\epsilon'_{yy}-\epsilon'_{zz})^2+(\epsilon'_{zz}-\epsilon'_{xx})^2,$$

$$T=\epsilon'^2_{xy}+\epsilon'^2_{yz}+\epsilon'^2_{zx},$$

and a_c, a_v, b, and d are the deformation potentials.

From Eq. (3) it follows that the conduction band is merely influenced by the hydrostatic deformation $\Sigma\epsilon_{ii}$, but the valence band undergoes an additional splitting $\Delta E_v^- - \Delta E_v^+$ due to tetragonal distortions and due to shear strain. The situation in strained 2D layers is comprehensively described, e.g., in Ref. 6 and we want to outline it only briefly. In the case of a quantum well, ΔE_v^- corresponds to the heavy hole (hh) and ΔE_v^+ to the light hole (lh) of the valence band. The change of the band gap for the e-hh transition is given by $\Delta E_c - \Delta E_v^-$. As all deformation potentials for ZnSe are negative (see Table I) and also $a=(a_c-a_v)<0$, a negative (compressive) hydrostatic deformation results in a positive shift of the conduction band, the valence band, and the band gap, too. On the other hand, the valence band splitting leads to a reduction of the e-hh transition energy in biaxially strained layers like $Cd_xZn_{1-x}Se$/ZnSe quantum wells. However, this reduction is not sufficient to compensate for the increase of the band gap due to the hydrostatic strain, because $Cd_xZn_{1-x}Se$ layers pseudomorphically grown on ZnSe or GaAs show a blueshift of the band gap compared to bulk material.[8] Vice versa, strain relaxation in wires is expected to cause a redshift with respect to the quantum well reference.

In Fig. 5(a), the energy shift of the conduction band and the valence band with respect to the compressively strained $Cd_{0.35}Zn_{0.65}Se$/ZnSe quantum well is shown as a function of x, with z fixed in the center of the quantum well. We have neglected piezoelectric effects, which are not expected to have dominant influence on the PL energy, even in narrow wires.[11] The values of the deformation potentials a, a_v, a_c, and b for ZnSe and cubic CdSe are listed in Table I. For $Cd_xZn_{1-x}Se$ we used linear interpolations. As the parameter d is not available for CdSe in zinc-blende formation, the ZnSe value $d=-3.8$ was taken in a first approximation. The change of the conduction band edge is only influenced by ϵ_{xx} and ϵ_{zz}, because ϵ_{yy} is independent of the wire width.

In wires, the relaxation process causes a shift of the conduction band to lower energies. This shift increases in narrow wires due to the stronger relaxation in the wire center as compared to wide ones. The laterally inhomogeneous strain distribution results in a more distinct shift of the conduction band at the wire sidewalls thus causing a substantial inhomogeneity in the conduction band energy of the wires. In principle the valence band shows a similar behavior. However, the variation of the energy between the center and the sidewalls of the wire is much less pronounced due to shear strain and due to the smaller value of a_v compared to a_c. From this result, a field enhanced transfer of the electrons to the energetically favorable regions at the sidewalls is expected, while the holes should be weakly confined in the center of the wire. It has to be noted that a substantial spreading of a_v and a_c can be found in the literature,[31,32] causing uncertainties in the lateral variation of conduction and valence band. However,

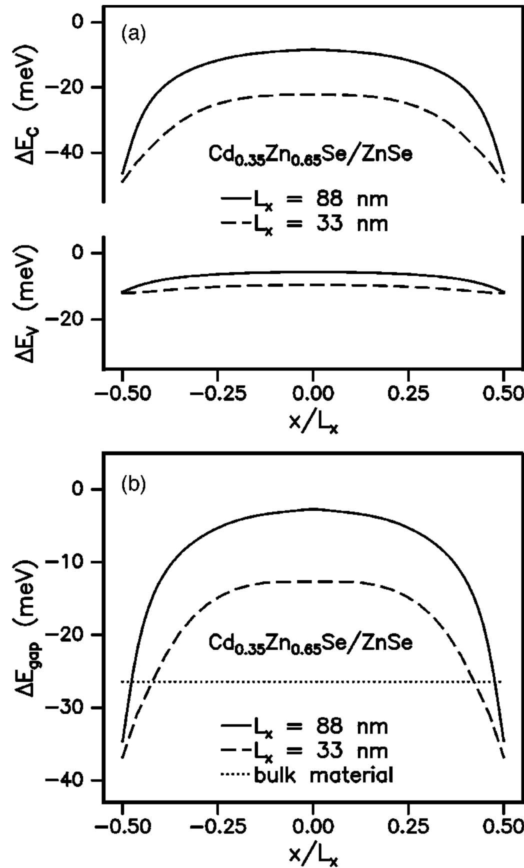

FIG. 5. Shift of the conduction and the valence band ΔE_c and ΔE_v, respectively [(a), top] and the band gap ΔE_{gap} [(b), bottom] in the $Cd_{0.35}Zn_{0.65}Se$/ZnSe system as a function of x with respect to a biaxially strained 2D reference. Solid line: wire width $L_x = 88$ nm, dashed line: $L_x = 33$ nm, dotted line (b): unstrained $Cd_{0.35}Zn_{0.65}Se$.

the calculated energy gap is rather reliable, because the deformation potential a is known quite exactly.

The shift of the energy gap for the e-hh transition $\Delta E_{gap} = \Delta E_c - \Delta E_v^-$ with respect to the compressively strained quantum well is shown at the bottom of Fig. 5(b) for different wires. The energy shift between the band gap of the strained layer, marked as $\Delta E_{gap} = 0$ on our scale, and the unstrained bulk material (dashed-dotted line) is about 21.8 meV. In wires, a redshift of the band gap is obtained, strongly inhomogeneous over the wire cross section and most pronounced in narrow wires. While, e.g., at the center of the wire the $L_x = 88$ nm wide wires exhibit a redshift of only 4 meV, the band-gap shift between the quantum well and the 33 nm wide wires is about 13 meV. In contrast, at the wire sidewalls the band-gap shift is nearly independent of the wire width and amounts to more than 30 meV. This reflects the minor influence of the wire width on the strain field at the sidewalls. It is worth mentioning that in a region of a few nm at the sidewalls the band gap of the wires is even smaller than in unstrained $Cd_xZn_{1-x}Se$ bulk material. This is mainly due to the shear strain component ϵ_{zx}, which reaches its maximum at the sidewalls and modifies the valence band according to Eq. (3).

V. DISCUSSION

In this section, some selected theoretical predictions are compared to experimental data obtained by PL spectroscopy.

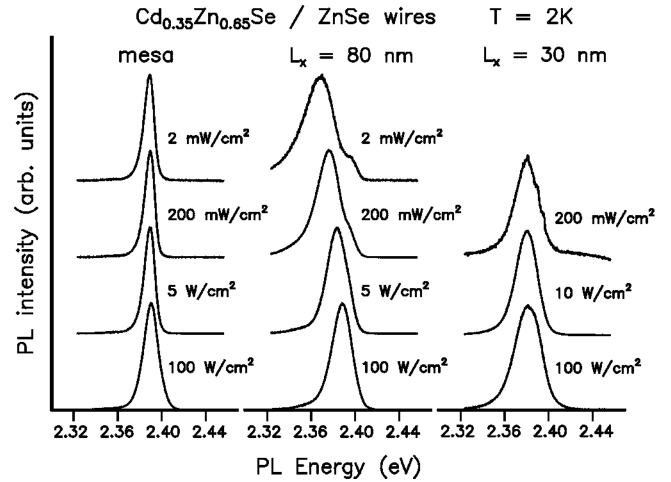

FIG. 6. PL spectra for a 2D reference (left), wires with $L_x = 80$ nm (center), and $L_x = 30$ nm (right) for different excitation power densities.

First, we discuss an experimental indication for the lateral inhomogeneity of the band gap. Subsequently, the size-dependent band gap variation due to strain and lateral quantization effects will be analyzed.

A. Lateral band-gap inhomogeneity in wires

In Fig. 6, PL spectra for the 2D reference, an 80 nm wide wire array, and wires with $L_x = 30$ nm are compared for different excitation densities ranging from 2 mW/cm^2 to 100 mW/cm^2.

In the case of the 2D reference, no significant change of the PL spectrum is observed by varying the excitation density by almost five orders of magnitude (see Fig. 6, left). There is only a slight broadening of the spectra for excitation densities above 10 W/cm^2 due to the saturation of localized states. Especially, there is no indication of defect related photoluminescence at low densities, indicating the high quality of the sample.

The situation is completely different in the case of the 80 nm wide wires (Fig. 6, center), where both the peak energy and the shape of the PL spectrum strongly depend on the excitation density. Increasing the excitation density from 2 mW/cm^2 to 100 W/cm^2, the PL maximum shifts by about 19 meV to the blue, while simultaneously the FWHM (full width at half maximum) of the PL spectrum decreases from 34 meV to about 22 meV. For an interpretation of these phenomena we follow the arguments given by Tan *et al.*,[12] taking into account the lateral inhomogeneity of the conduction and the valence band in wires due to partial strain relaxation. As discussed above (see Fig. 5), the sidewalls are energetically favorable especially for the electrons, resulting in a reduction of the band gap in the vicinity of the wire sidewalls. For low excitation densities, these energetically lower states are expected to be populated efficiently, contributing significantly to the PL spectrum. Due to the averaging of the PL signal over the cross section of the wires, the FWHM is enhanced compared to the 2D reference. At high excitation densities the recombination in the center region of the wire dominates the PL spectrum due to the successive filling of the low energy states at the wire sidewalls. As a consequence

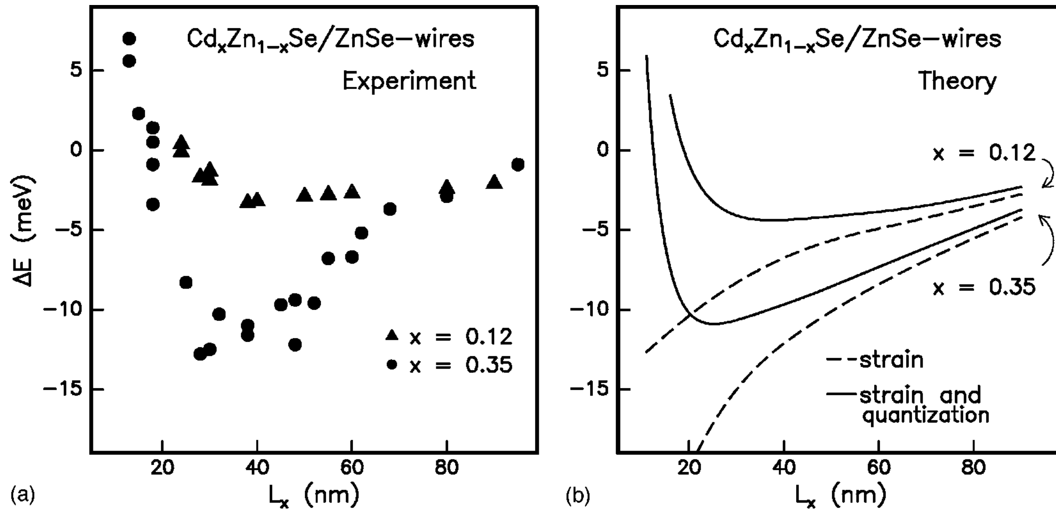

FIG. 7. Experimental [(a), left] and theoretical [(b), right] PL energy shifts with respect to a 2D reference for $Cd_xZn_{1-x}Se/ZnSe$ wires with $x=0.12$ and $x=0.35$ versus the lateral wire width L_x. Dashed lines in (b): energy shift due to strain relaxation, solid lines: energy shift due to strain relaxation and lateral confinement.

both a shift of the PL maximum to higher energies and a reduction of the FWHM is expected, in agreement with the experimental data.

In contrast, the change of the PL energy and the PL line shape with excitation power is suppressed for narrow ($L_x=30$ nm) wires (see Fig. 6, right). This reflects on the one hand the smaller variation of the band gap across the wires for decreasing wire width (see Fig. 5). On the other hand, lateral confinement effects have to be taken into account in such narrow structures, resulting in fixed eigenenergies across the wires. Consequently, no significant energy shift and line shape change with varying excitation density is expected in narrow quantum wires, in agreement with our experimental findings. The enhanced PL linewidth compared to the 2D reference is most likely caused by a spatial variation of the lateral quantization energy due to size fluctuations.[33]

B. Size dependence of the PL energy

In order to discuss the wire width dependence of the PL energy in the light of our model calculations, we performed PL measurements at a relatively high excitation power density of 100 W/cm^2. This guarantees a sufficient carrier density in the wire in order to suppress the influence of strain induced carrier localization in the vicinity of the sidewalls as discussed above. In Fig. 7(a), the shift of the peak energy of the PL signal with respect to the 2D reference is plotted versus the wire size for both $Cd_{0.12}Zn_{0.88}Se/ZnSe$ (triangles) and $Cd_{0.35}Zn_{0.65}Se/ZnSe$ wires (circles). The two regimes revealing a different behavior concerning the size-dependent energy shift mentioned in Sec. III become very clear. For wire widths larger than 30 nm the strain relaxation in $Cd_{0.35}Zn_{0.65}Se/ZnSe$ wires leads to a redshift of the PL signal of more than 10 meV with decreasing width. In the case of the $Cd_{0.12}Zn_{0.88}Se/ZnSe$ wires this effect is less pronounced, because of the smaller compressive strain in this system. On the contrary, a substantial shift of the transition energy to higher energies due to lateral quantization effects is observed for narrow wires.

In Fig. 7(b), the size-dependent energy shift of the band gap caused by strain relaxation calculated for the center of the wire is depicted for $Cd_xZn_{1-x}Se/ZnSe$ wires with $x=0.35$ (lower dashed line) and $x=0.12$ (upper dashed line). The calculations predict a strong redshift when reducing the wire width from 100 nm to 10 nm. Of course, the change of the band gap is less pronounced for $x=0.12$, as the strain in the 2D layer is smaller than in the case of the $Cd_{0.35}Zn_{0.65}Se/ZnSe$ quantum well. As can be seen easily by a comparison between the experimental data and the model calculations, no agreement can be obtained for wire widths below 40 nm because of the increasing influence of lateral confinement effects in such narrow wires. Therefore we took into account the lateral quantization energy using a finite square well potential,[21] which results in a blueshift of the band gap with decreasing size. For the electron and the heavy hole mass again linear interpolations between the values for ZnSe and CdSe (see Table I) were used. Because the lateral confinement affects the in-plane motion of the holes, we evaluated the in-plane heavy hole mass $m_{hh,\parallel}$ for $Cd_xZn_{1-x}Se$ using the Luttinger-Kohn parameters.[34] Taking into account both the band-gap shift due to strain relaxation and lateral carrier confinement [solid lines in Fig. 7(b)], a reasonable agreement between the experimental data and the model calculations is obtained. It is important to note that no fit parameters are used for the theoretical curve.

While this agreement is rather good in the size regime larger than about 30 nm, some deviations have to be discussed for the narrowest wires. As can be seen, the blueshift of the PL signal in narrow wires is more distinct than predicted by the theory. Our calculations show that the strain release should continue down to the sub-20-nm regime with a saturation not above 10 nm. However, as discussed in Sec. III, the Raman data indicate no substantial strain relaxation for wire widths below 30 nm. Thus both experiments, PL and Raman spectroscopy, give an indication that the relaxation in the deeply etched narrow wires is more efficient than predicted by theory. This discrepancy is not fully understood yet. A reason for this phenomenon might be on the one hand the etch profile in these structures, which is not perfectly rectangular shaped. On the other hand, the sidewall roughness of about 3 nm in the wet etched patterns may modify

the strain relaxation mechanism. This effect would play an important role especially in very narrow wires, where a relatively large fraction of the structure is in the vicinity of the sidewalls.

VI. CONCLUSION

Quantum wires fabricated by lateral patterning of compressively strained $Cd_xZn_{1-x}Se/ZnSe$ quantum well structures have been studied both experimentally and theoretically as a model system to evaluate the size dependence of strain relaxation and lateral carrier confinement effects. Photoluminescence measurements have been performed to investigate the variation of the band gap with decreasing wire size. In addition, Raman experiments gave insight into the change of the lattice constant by monitoring the size-dependent shift of the $Cd_xZn_{1-x}Se$ LO frequency. The experimental data have been compared to model calculations of the size-dependent band gap taking into account strain relaxation as well as lateral carrier confinement.

From our calculations we conclude (i) the strain relaxation in deep etched compressively strained $Cd_xZn_{1-x}Se/ZnSe$ wires is strongly inhomogeneous, causing a variation of the conduction and the valence band across the wire cross section and (ii) the strain relaxation results in a redshift of the band gap with decreasing size.

An experimental indication of the lateral inhomogeneity of the conduction and the valence band was found at extremely low excitation densities, where the spatial separation of electrons and holes is evident by an energetically broadened photoluminescence signal, shifted to lower energy. As a main result, however, the redshift observed experimentally for the band gap and the $Cd_xZn_{1-x}Se$ LO phonon frequency with decreasing wire width indicates a size-dependent lattice distortion due to strain relaxation for large wires. A good agreement is achieved between the PL data and the theoretical calculations for wire widths down to 40 nm, explaining the observed redshift of the PL maximum with respect to the 2D reference of more than 10 meV for wires with a high ($x=35\%$) and 3 meV for wires with a low ($x=12\%$) Cd content. While the theory predicts a progressing strain relaxation down to wire widths in the 10 nm range, our experimental data indicate a saturation of the strain release for wire widths below 30 nm, possibly caused by the influence of etch profile and sidewall roughness on the strain relaxation process. In narrow wires, lateral quantization effects have to be taken into account to model the observed blueshift of the PL signal.

ACKNOWLEDGMENTS

We would like to thank D. Eisert for fruitful discussion and acknowledge the financial support of the Deutsche Forschungsgemeinschaft.

*Electronic address: kuemmell@physik.uni-wuerzburg.de
†Present address: Institut für Festkörperphysik, Universität Bremen, 28359 Bremen, Germany.

[1] J. W. Matthews and A. E. Blakeslee, J. Cryst. Growth **27**, 118 (1974).
[2] I. Vurgaftman, J. M. Hinckley, and J. Singh, IEEE J. Quantum Electron. **30**, 75 (1994).
[3] L. F. Tiemeijer, P. Thijs, P. de Waard, J. Birsma, and T. v. Dongen, Appl. Phys. Lett. **58**, 2738 (1991).
[4] J. Hashimoto, T. Katsuyama, I. Yoshida, and H. Hayashi, IEEE J. Quantum Electron. **29**, 1863 (1993).
[5] P. Ru, W. Chow, J. Moloney, and S. Koch, Appl. Phys. Lett. **64**, 1469 (19994).
[6] T. P. Pearsall, F. Pollak, J. C. Bean, and R. Hull, Phys. Rev. B **33**, 6821 (1986).
[7] T. Y. Wang and G. B. Stringfellow, J. Appl. Phys. **67**, 344 (1990).
[8] H. J. Lozykowski and V. K. Shastri, J. Appl. Phys. **69**, 3235 (1991).
[9] R. J. Thomas, B. Rockwell, H. R. Chandrasekhar, M. Chandrasekhar, A. K. Ramdas, M. Kobayashi, and R. L. Gunshor, J. Appl. Phys. **78**, 6569 (1995).
[10] J. Wang, X. Wang, Z. Q. Zhu, and T. Yao, J. Phys.: Condens. Matter **7**, 5835 (1995).
[11] Y.M. Niquet, C. Priester, and H. Mariette, Phys. Rev. B **55**, R7387 (1997).
[12] I-H. Tan, R. Mirin, T. Yasuda, E. L. Hu, J. Bowers, C. B. Prater, P. K. Hansma, M. Y. He, and A. G. Evans, J. Vac. Sci. Technol. B **10**, 1971 (1992).
[13] H. Straub, G. Brunthaler, W. Faschinger, G. Bauer, and C. Vieu, Acta Phys. Pol. A **90**, 1085 (1996).
[14] M. Notomi, J. Hammersberg, H. Weman, S. Nojima, H. Sugiura, M. Okamoto, T. Tamamura, and M. Potemski, Phys. Rev. B **52**, 11 147 (1995).
[15] M. Grundmann, O. Stier, and D. Bimberg, Phys. Rev. B **52**, 11 969 (1995).
[16] L. De Caro and L. Tapfer, Phys. Rev. B **51**, 4381 (1995).
[17] Y.-P. Chen, J. D. Reed, W. J. Schaff, and L. F. Eastman, Appl. Phys. Lett. **65**, 2202 (1994).
[18] S. C. Jain, A. H. Harker, A. Atkinson, and K. Pinardi, J. Appl. Phys. **78**, 1630 (1995).
[19] S. C. Jain, B. Dietrich, H. Richter, A. Atkinson, and A. H. Harker, Phys. Rev. B **52**, 6247 (1995).
[20] K. Nishi, A. A. Yamaguchi, J. Ahopelto, A. Usui, and H. Sakaki, J. Appl. Phys. **76**, 7437 (1994).
[21] M. Illing, G. Bacher, T. Kümmell, A. Forchel, T. G. Andersson, D. Hommel, B. Jobst, and G. Landwehr, Appl. Phys. Lett. **67**, 124 (1995).
[22] M. A. Haase, J. Qiu, J. M. DePuydt, and H. Cheng, Appl. Phys. Lett. **59**, 1272 (1991).
[23] S. Taniguchi, T. Hino, S. Itoh, K. Nakano, N. Nakayama, A. Ishibashi, and M. Ikeda, Electron. Lett. **32**, 552 (1996).
[24] *Physics of II-VI and I-VII-Compunds, Semimagnetic Semiconductors*, edited by O. Madelung, Landolt-Börnstein, New Series, Group III, Vol. 17, pt. b (Springer, Berlin, 1982).
[25] C. D. Lee, B. K. Kim, J. W. Kim, H. L. Park, C. H. Chung, S. K. Chang, J. I. Lee, and C. K. Noh, J. Cryst. Growth **138**, 136 (1994).
[26] G. Bacher, D. Tönnies, D. Eisert, A. Forchel, M. O. Möller, M. Korn, B. Jobst, D. Hommel, G. Landwehr, J. Söllner, and M. Heuken, J. Appl. Phys. **79**, 4368 (1996).
[27] M. Illing, G. Bacher, T. Kümmell, A. Forchel, D. Hommel, B. Jobst, and G. Landwehr, J. Vac. Sci. Technol. B **13**, 2792 (1995).
[28] G. Lermann, T. Bischof, A. Materny, W. Kiefer, T. Kümmell, G. Bacher, A. Forchel, and G. Landwehr, J. Appl. Phys. **81**, 1446 (1997).

[29] R. G. Alonso, E.-K. Suh, A. K. Ramdas, N. Smarth, H. Luo, and J. K. Furdyna, Phys. Rev. B **40**, 3720 (1989).
[30] G. E. Pikus and G. L. Bir, Sov. Phys. Solid State **1**, 1502 (1960) [Fiz. Tverd. Tela (Leningrad) **1**, 1642 (1958)].
[31] A. Blacha, H. Presting, and M. Cardona, Phys. Status Solidi B **126**, 11 (1984).
[32] S. Lankes, T. Reisinger, B. Hahn, C. Meier, M. Meier, and W. Gebhardt, J. Cryst. Growth **159**, 481 (1996).
[33] P. Ils, M. Michel, A. Forchel, I. Gyuro, M. Klenk, and E. Zielinsky, Appl. Phys. Lett. **64**, 496 (1994).
[34] J. M. Luttinger and W. Kohn, Phys. Rev. **97**, 869 (1955).
[35] G. Schötz, W. Sedlmaier, M. Lindner, and W. Gebhardt, J. Phys.: Condens. Matter **7**, 795 (1995).
[36] B. Rockwell, H. R. Chandrasekhar, M. Chandrasekhar, A. M. Ramdas, M. Kobayashi, and R. L. Gunshor, Phys. Rev. B **44**, 11 307 (1991).
[37] H. W. Hölscher, A. Nöthe, and C. H. Uihlein, Phys. Rev. B **31**, 2379 (1985).